

International Journal of Advances in Pharmaceutical Analysis

IJAPA Vol. 1 Issue 1 (2011) 10-15

Journal Home Page <http://www.ss-journals.com/index.php/ijapa>

DETERMINATION OF OPTICAL CONSTANTS AND OPTICAL BAND GAP IN $\text{Ge}_{40}\text{Te}_{60-x}\text{Sb}_x$ THIN FILMS

S. Shukla, S. Kumar*

Department of Physics, Christ Church College, Kanpur-208001, India

ABSTRACT

The optical transmission spectra of thin films of $\text{Ge}_{40}\text{Te}_{60-x}\text{Sb}_x$ ($x = 0, 2, 4, 6$ and 10), prepared by vacuum evaporation technique from their corresponding bulk samples, are recorded over the spectral region of $500\text{--}2700$ nm. A simple straight forward method proposed by Swanepoel has been applied to determine various optical parameters like refractive index (n), extinction coefficient (k), absorption coefficient (α), real and imaginary dielectric constants (ϵ' & ϵ'') in the measured range of wavelength. The optical band gap (E_g) has also been calculated by Tauc's relation. It has been found that the E_g and n decreases with Sb concentration in $\text{Ge}_{40}\text{Te}_{60-x}\text{Sb}_x$ system.

Keywords: Chalcogenides; Optical constants; Optical band gap; Thin films

1. Introduction

The modern technological applications of chalcogenide glasses are widespread specifically as moldable infrared optics including lenses and infrared optical fibers as these materials transmit across the full range of the infrared regime of the electromagnetic spectrum. Integrated optics is increasingly being viewed as an important step in the development of modern telecommunications systems. The chalcogenide glasses are promising materials for use in the guided wave devices integrated optics, optical data storage and infrared telecommunication systems^{1,2}. The structure of chalcogenide glasses exhibiting memory switching usually consists of long chalcogen chains in which atomic rearrangements occur easily³. They possess high electrical conductance, which can result in large power dissipation.

Modern chalcogenide compounds like Ge-Sb-Te, widely used in rewritable optical disks and PRAM devices, are fragile glass-formers; therefore they are able to crystallize in about 100 ns⁴⁻¹¹. Therefore these alloys are used for data recording based on the rapid and reversible amorphous-to-crystalline phase

transformation^{12,13} that is accompanied by increase in the optical reflectivity and the electrical conductivity. However, uncertainties about the optical band gaps and electronic transport properties of these phases have persisted because of inappropriate interpretation of reported data and the lack of definitive analytical studies.

The optical band gap, refractive index and extinction coefficient are the most significant parameters in amorphous semiconducting thin films. The optical behavior of a material is utilized to determine its optical constants. Films are ideal specimens for reflectance and transmittance type measurements. Therefore, an accurate measurement of the optical constants is extremely important. Chalcogenide glasses have been found to exhibit the change in refractive index¹⁴⁻¹⁶ under the influence of light, which makes it possible to use these materials to record not only the magnitude but also the phase of illumination.

In the view of the above, here we report the determination of optical constants and optical band gap in $\text{Ge}_{40}\text{Te}_{60-x}\text{Sb}_x$ ($x = 0, 2, 4, 6$ and 10) thin films. A relative simple method for determining various optical

constants, using only transmission spectra, based upon Swanepoel's method^{17,18} has been used. Section 2 and 3 describes the experimental details and the results respectively. The conclusions have been presented in the last section.

2. Experimental details

Bulk samples of $\text{Ge}_{40}\text{Te}_{60-x}\text{Sb}_x$ ($x = 0, 2, 4, 6$ and 10) system were prepared by melt quenched technique. High purity (99.999 % pure) elements, Germanium, Antimony and Tellurium were weighed by electronic balance (Shimadzu, AUX 220) according to their atomic percentages, with a least count of 10^{-4} gm. The properly weighed materials were put into clean quartz ampoules (length ~ 5 cm and internal diameter ~ 8 mm) and then sealed under vacuum of 1.3×10^{-3} Pa. These sealed ampoules were heated in electric furnace up to 1400°C and kept at that temperature for 10 - 12 hours. The temperature of the furnace was raised slowly at a rate of $3 - 4^\circ\text{C}/\text{min}$. During the heating process ampoules were constantly rocked, by rotating a ceramic rod to which the ampoules were tucked away in the furnace. This was done to obtain homogenous glassy alloy. After rocking for about 10 hours, as obtained molten materials were rapidly quenched by removing the ampoules from the furnace and dropping into ice-cooled water. The quenched samples of the glassy alloys were taken out by breaking the quartz ampoules. The amorphous to polycrystalline nature of the samples with increase of Sb concentration in $\text{Ge}_{40}\text{Te}_{60}$ alloy were ascertained by the X-ray diffraction pattern as shown in Fig. 1. Compositional analysis was performed using electron probe micro-analysis (EPMA) technique.

Thin films of $\text{Ge}_{40}\text{Te}_{60-x}\text{Sb}_x$ ($x = 0, 2, 4, 6$ and 10) alloys were prepared by vacuum evaporation technique keeping glass substrate at room temperature. The thin films were kept in the deposition chamber in the dark for 24 hours before using them. This was done to allow sufficient

annealing at room temperature so that a metastable thermodynamic equilibrium may be attained in the samples as suggested by Abkowitz¹⁹. The optical transmission spectra of thin films of $\text{Ge}_{40}\text{Te}_{60-x}\text{Sb}_x$ were measured by a double beam UV-VIS-NIR computer controlled spectrophotometer (Perkin-Elmer, model Lambda-750) as a function of wavelength of the incident light. The spectrophotometer was set with a suitable slit width of 1nm in the measured spectral range. The interference effects give rise to the spectrum showed a maxima and minima of the transmission curve. These interference fringes could be used to calculate various optical parameters.

3. Results and discussion

3.1. Determination of refractive index and extinction coefficient: Fig. 2 shows the transmission spectra as a function of wavelength for thin films of $\text{Ge}_{40}\text{Te}_{60-x}\text{Sb}_x$ ($x = 0, 2, 4, 6$ and 10) system. The various optical parameters were determined using Swanepoel's method which is based on the idea of Manifacier *et al.*²⁰ of creating upper and lower envelopes of the optical transmission spectra. The refractive index, n of the film in the transparent region ($\alpha = 0$) is given by:

$$n = [N + (N^2 - s^2)^{1/2}]^{1/2} \quad (1)$$

Where

$$N = (2s/T_m) - (s^2 + 1)/2 \quad (2)$$

Where T_m is the envelope values at the wavelengths in which the lower envelope and the experimental transmission spectrum are tangent and s is the refractive index of the substrate.

In the region of weak and medium absorption, where $\alpha \neq 0$, transmittance decreases mainly due to the effect of absorption coefficient (α) and Eq.(2) modifies to:

$$N = [2s(T_M - T_m) / T_M T_m] + (s^2 + 1)/2 \quad (3)$$

Where T_M is the envelope values at the wavelengths in which the upper envelope and the experimental transmission spectrum are tangent.

If n_1 and n_2 are the refractive indices of two adjacent maxima or two adjacent minima at wavelengths λ_1 and λ_2 , respectively, then according to the basic equation for interference fringes:

$$2nd = m\lambda \quad (4)$$

where 'm' is an order number. d is the thickness of the thin film which is given by:

$$d = \lambda_1 \lambda_2 / 4(\lambda_1 n_2 - \lambda_2 n_1) \quad (5)$$

It should be noted that owing to optical absorption, this particular equation is not valid at the interference maxima and minima, but is valid at the tangent points referred to [17]. Using equation (4), new more precise values of the refractive index could be determined by a procedure which was explained in detail in [17, 18].

The extinction coefficient k, which is a measure of fraction of light lost due to scattering and absorption per unit distance of the participating medium is calculated by the relation $x = \exp(-4\pi kd/\lambda)$. The absorbance, x is given in terms of the interference extremes using the following relation [17]:

$$x = [E_m - \{E_m^2 - (n^2 - 1)^3(n^2 - s^4)\}^{1/2}] / [(n - 1)^3(n - s^2)] \quad (6)$$

Where

$$E_m = [(8n^2s / T_m) - (n^2 - 1)(n^2 - s^2)] \quad (7)$$

The variation of n and k with wavelength for different compositions of $\text{Ge}_{40}\text{Te}_{60-x}\text{Sb}_x$ system are shown in Fig. 3 and 4, respectively. It is clear from these figures that n and k decreases with an increase in λ . This behavior is due to increase in transmittance and decrease of absorption coefficient with λ . The decrease in refractive index with wavelength shows the normal dispersion behavior of the material. The calculated values of n and k for thin films under study at $\lambda = 1650$ nm are given in Table 1.

3.2 Determination of dielectric constants:

The real (ϵ') and imaginary (ϵ'') parts of the dielectric constants can be estimated if the refractive index and extinction coefficient are known from the relation:

$$\epsilon' = n^2 - k^2 \quad (8)$$

and

$$\epsilon'' = 2nk \quad (9)$$

The values of ϵ' and ϵ'' for $\text{Ge}_{40}\text{Te}_{60-x}\text{Sb}_x$ thin films are calculated with the help of Eq. (8) and (9). The variation of ϵ' and ϵ'' with λ for different samples under study is shown in Fig. 5 and 6 respectively. It is evident from these figures that variation of ϵ' and ϵ'' with λ follows the same trend as followed by n and k. The composition dependence of ϵ' and ϵ'' are also listed in Table 1 for glassy system used in the present study.

3.3 Determination of absorption coefficient (α) and optical band gap (E_g):

The absorption coefficient (α) of the $\text{Ge}_{40}\text{Te}_{60-x}\text{Sb}_x$ thin films can be calculated from the values of extinction coefficient (k) and λ using the well known formula $k = \alpha\lambda / 4\pi$. A plot of α as a function of photon energy (hv) is illustrated in Fig. 7 and is found to increase with increase in hv. The calculated values of α at a particular wavelength $\lambda = 1650$ nm for different compositions is also listed in Table 2.

In chalcogenide glasses, the optical absorption edge spectra generally contain three distinct regions¹⁸:

(i) High absorption region ($\alpha = 10^4 \text{ cm}^{-1}$), which involves the optical transition between valence band and conduction band and determines the optical band gap. The absorption coefficient in this region is given by:

$$\alpha \nu h = B (h\nu - E_g)^p \quad (10)$$

where E_g is defined as optical energy gap and B is a constant related to band tailing parameter. In the above mentioned equation, $p = 1/2$ for a direct allowed transition, $p = 3/2$ for a direct forbidden transition, $p = 2$ for an indirect allowed transition and $p = 3$ for an indirect forbidden transition.

(ii) For α less than about $\sim 10^4 \text{ cm}^{-1}$ there is usually an Urbach tail where α depends exponentially on the photon energy and is given by:

$$\alpha \nu h = \alpha_0 \exp(h\nu / E_c), \quad (11)$$

where α_0 is a constant and E_e is the width of the band tail of localized states in the band gap which generally represents the degree of disorder in amorphous semiconductor.

(iii) The region ($\alpha \leq 10^2 \text{ cm}^{-1}$) involves low energy absorption and originates from defects and impurities.

The analysis of the absorption coefficient has been carried out to obtain the optical band gap (E_g). The E_g has been determined from absorption coefficient data as a function of photon energy ($h\nu$), using the Eq.(10). After fitting all the values of p in the Tauc's relation, the value of p equals to 2 is found to hold good leading to indirect transitions²¹. The graph between $(\alpha h\nu)^{1/2}$ and $h\nu$ for $\text{Ge}_{40}\text{Te}_{60-x}\text{Sb}_x$ films is shown in the Fig. 8. The non-linear nature of the graph provides evidence that the transition in the forbidden gap is of indirect type. The values of E_g are given in Table.2 for the samples under consideration. It is clear from the table that optical band gap decreases with Sb content. The decrease in optical band gap with increase in Sb concentration may be due to the increase in the amount of disorder in the binary material and hence increase in the density of defect states.

Conclusion

The optical transmission spectra of thin films of $\text{Ge}_{40}\text{Te}_{60-x}\text{Sb}_x$ ($x = 0, 2, 4, 6$ and 10) are measured in the wavelength range 500-2700 nm by spectrophotometer. Various optical parameters have been calculated by Swanepoel method using optical transmission data. The values of n , k , ϵ' and ϵ'' is found to be decrease with increase in wavelength. A decrease in n and E_g with Sb content is also being observed which could be correlated with increase in the density of defect states.

Acknowledgement

We are very much grateful to Department of science and technology (DST), New Delhi for providing us financial assistance

as a major research project during the span of this work.

References

1. A.V. Stronski, G. Harman, P. Mach (Eds.), Proceedings of the NATO Advanced Research Workshop on Micro-electronic Inter Connections and Assembly, Kluwer Academic Press, The Netherlands, 1998.
2. P. Sharma, S.C. Katyal, Thickness dependence of optical parameters for Ge-Se-Te thin films. Mater. Lett. 2007; 61: 4516-4518.
3. S.R. Ovshinsky, K. Sapru, W.E. Spear, (Eds.), Proceedings of the Seventh International Conference on Amorphous and Liquid Semiconductors, Institute of Physics, Bristol, 1977: 447.
4. S. R. Ovshinsky, P. H. Klose, Amorphous semiconductors for switching, memory, and imaging applications J. Non-Cryst. Solids 1972; 8-10: 892.
5. J. R. Boonell, C. B. Thomas, Solid State Electron 15 (1972) 1261.
6. J. Cornet, Ann.Chim 10 (1975) 239.
7. J. Colmenero and J. M. Barandiaran, J.non-Cryst.Solids 30 (1979) 263.
8. C. B. Thomas, A. Feltz, J. Non-Cryst.Solids 86 (1986) 33.
9. S. Asokan, G. Parthasarathyand, E. S. R. Gopal, J.Non-Cryst.Solids 86 (1986) 48.
10. C. B. Thomas, A. Feltz, J.Non-Cryst. Solids 86 (1986) 41.
11. N.Ziani, M. Blhedji, L. Heireche, Z. Bouchour, Blebachir, Physica B 358 (2005) 132.
12. N. Yamada, E. Ohno, N. Akahira, K. Nishiuchi, K. Nagata, M. Takao, Jpn. J. Appl. Phys. Suppl., Part 1 26-4 (1987) 61.
13. N. Yamada, E. Ohno, K. Nishiuchi, N. Akahira, M. Takao, J. Appl. Phys. 69 (1991) 2849.
14. V. Pandey, S. K. Tripathi, A. Kumar, J. Ovonic Research 3 (2007) 29.

15. S. Srivastava, V. Pandey, S. K. Tripathi, R. K. Shukla, A. Kumar, J. Ovonic Research 4 (2008) 83.
 16. A. Ahmad, S. A. Khan, K. Sinha, L. Kumar, Z. H. Khan, M. Zulfequar, M. Husain, Vacuum 82 (2008) 608.
 17. R. Swanepoel, J. Phys. E: Sci. Instrum. 17 (1984) 896.
 18. R. Swanepoel, J. Phys. E 16 (1983) 1214.
 19. M. Abkowitz, Polymer Eng. Sci. 24 (1984) 1149.
 20. J.C. Manifacier, J. Gasiot, J.P. Fillard, J. Phys. E: Sci. Instrum. 9 (1976) 1002.
 21. J. Tauc, The Optical Properties of Solids, North-Holland, Amsterdam, 1970.

Table 1 Refractive index (n), extinction coefficient (k), real and imaginary dielectric constants (ϵ' & ϵ'') for $\text{Ge}_{40}\text{Te}_{60-x}\text{Sb}_x$ thin films

| <i>Samples</i> | <i>Refractive index (n)</i> | <i>Extinction coefficient (k)</i> | <i>Real dielectric constant (ϵ')</i> | <i>Imaginary dielectric constant (ϵ'')</i> |
|--|-----------------------------|-----------------------------------|--|--|
| $\text{Ge}_{40}\text{Te}_{60}$ | 6.01 | 18.61×10^{-2} | 36.03 | 2.23 |
| $\text{Ge}_{40}\text{Te}_{58}\text{Sb}_2$ | 3.40 | 17.14×10^{-2} | 11.53 | 1.17 |
| $\text{Ge}_{40}\text{Te}_{56}\text{Sb}_4$ | 2.73 | 20.56×10^{-2} | 7.40 | 1.12 |
| $\text{Ge}_{40}\text{Te}_{54}\text{Sb}_6$ | 3.25 | 23.24×10^{-2} | 10.51 | 1.51 |
| $\text{Ge}_{40}\text{Te}_{50}\text{Sb}_{10}$ | 3.00 | 36.53×10^{-2} | 8.90 | 2.20 |

Table 2 Values of optical band gap and absorption coefficient (α) for $\text{Ge}_{40}\text{Te}_{60-x}\text{Sb}_x$ thin films

| <i>Samples</i> | <i>Optical band gap (E_g) in eV</i> | <i>Absorption coefficient (α) in cm^{-1} at 1650 nm</i> |
|--|--|---|
| $\text{Ge}_{40}\text{Te}_{60}$ | 0.70 | 1.42×10^4 |
| $\text{Ge}_{40}\text{Te}_{58}\text{Sb}_2$ | 0.62 | 1.30×10^4 |
| $\text{Ge}_{40}\text{Te}_{56}\text{Sb}_4$ | 0.59 | 1.56×10^4 |
| $\text{Ge}_{40}\text{Te}_{54}\text{Sb}_6$ | 0.56 | 1.77×10^4 |
| $\text{Ge}_{40}\text{Te}_{50}\text{Sb}_{10}$ | 0.52 | 2.78×10^4 |

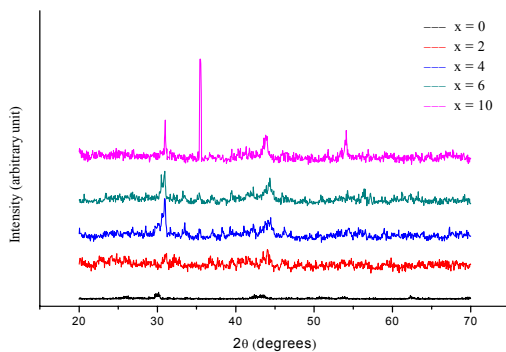


Fig. 1. X-ray diffraction pattern of $\text{Ge}_{40}\text{Te}_{60-x}\text{Sb}_x$ ($x = 0, 2, 4, 6$ and 10) alloys.

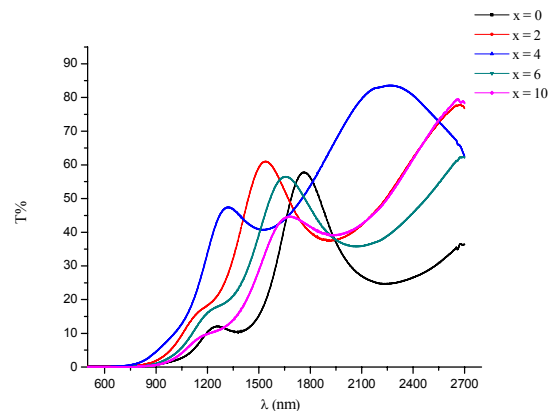


Fig. 2. Variation of the transmittance (T) with wavelength (λ) in $\text{Ge}_{40}\text{Te}_{60-x}\text{Sb}_x$ thin films.

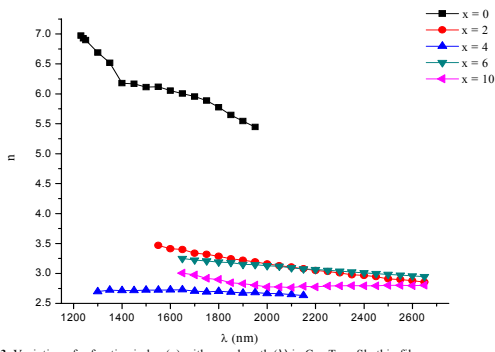


Fig. 3. Variation of refractive index (n) with wavelength (λ) in $Ge_{40}Te_{60-x}Sb_x$ thin films.

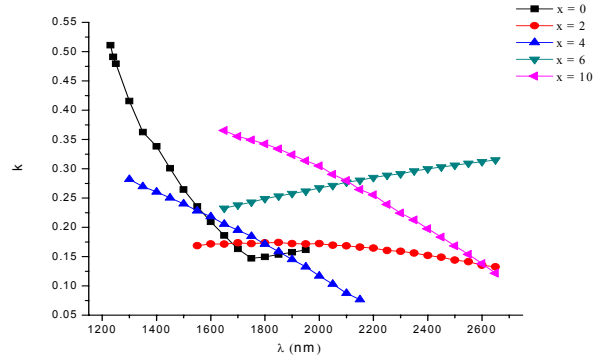


Fig. 4. Variation of extinction coefficient (k) with wavelength (λ) in $Ge_{40}Te_{60-x}Sb_x$ thin films.

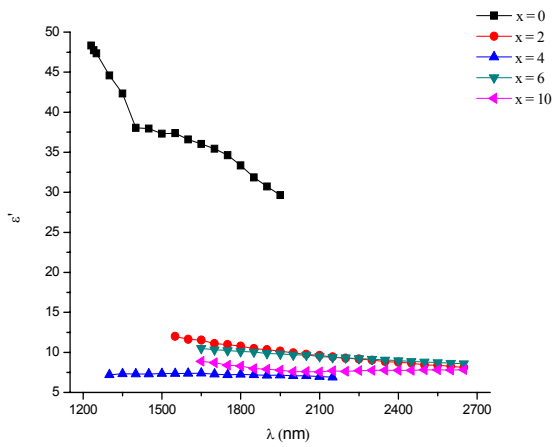


Fig. 5. Variation of real dielectric constant (ϵ') with wavelength (λ) in $Ge_{40}Te_{60-x}Sb_x$ thin films.

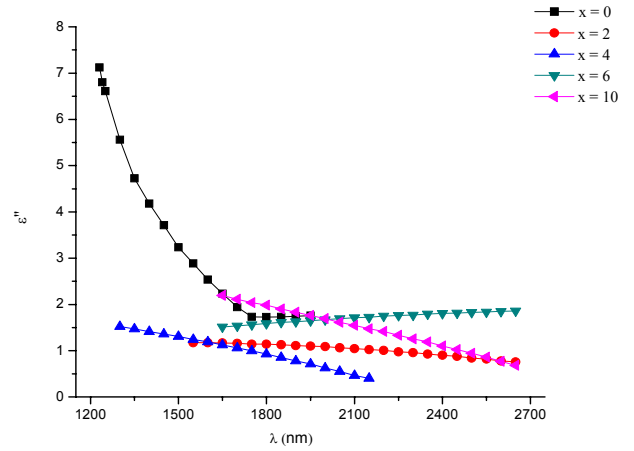


Fig. 6. Variation of imaginary dielectric constant (ϵ'') with wavelength (λ) in $Ge_{40}Te_{60-x}Sb_x$ thin films.

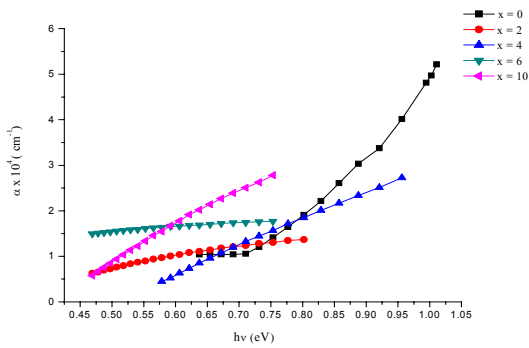


Fig. 7. Absorption coefficient (α) against photon energy (hv) in $Ge_{40}Te_{60-x}Sb_x$ thin films.

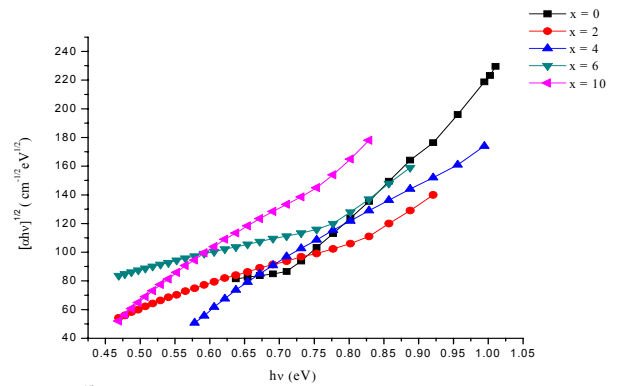


Fig. 8. $[\alpha hv]^{1/2}$ against photon energy (hv) in $Ge_{40}Te_{60-x}Sb_x$ thin films.